



OPEN ACCESS

Souradeep Bhattacharya, University of Hertfordshire, United Kingdom

Luis Angel Gutierrez Soto, Instituto de Fisica-Universidade Federal do Rio Grande do Sul, Brazil

*CORRESPONDENCE Paolo Ventura, □ paolo.ventura@inaf.it

RECEIVED 19 September 2025 REVISED 21 October 2025 ACCEPTED 21 October 2025 PUBLISHED 07 November 2025

Ventura P, Tosi S, Dell'Agli F and Bianchi S (2025) Planetary nebulae: a key tool to reconstruct the evolutionary history of stars. Front. Astron. Space Sci. 12:1709148. doi: 10.3389/fspas.2025.1709148

COPYRIGHT

© 2025 Ventura, Tosi, Dell'Agli and Bianchi. This is an open-access article distributed under the terms of the Creative Commons Attribution License (CC BY). The use, distribution or reproduction in other forums is permitted, provided the original author(s) and the copyright owner(s) are credited and that the original publication in this journal is cited, in accordance with accepted academic practice. No use, distribution or reproduction is permitted which does not comply with these terms.

Planetary nebulae: a key tool to reconstruct the evolutionary history of stars

Paolo Ventura^{1*}, Silvia Tosi¹, Flavia Dell'Agli¹ and Stefano Bianchi²

¹INAF, Osservatorio Astronomico di Roma, Rome, Italy, ²Dipartimento di Matematica e Fisica, Università degli Studi Roma Tre, Roma, Italy

Planetary nebulae, among the most fascinating objects in the sky, have been extensively investigated in the past years, because their study provides important information on the low and intermediate mass stellar populations of the host environment, formed earlier than ~100 Myr ago. We report on the recent progresses achieved in the study of this class of objects, regarding the dust and gas content of the nebula, which allows us to reconstruct the dust formation process occurred during the previous asymptotic giant branch phase, and the chain of events occurred since the stars leave the asymptotic giant branch until the planetary nebula stage. The possibility offered by these studies to assess the role played by the stars of low and intermediate mass as dust manufactures in the Universe is also commented.

KEYWORDS

planetary nebulae: general, planetary nebulae: individual, stars: AGB and post-AGB, stars: abundances, stars: carbon, stars: evolution

1 Introduction

Planetary Nebulae (hereafter PN) represent a relatively short, yet extremely interesting evolutionary phase crossed by the stars of initial mass below $\sim 8\,M_{\odot}$, on their way to the final cooling, towards the white dwarf stage. Their study received a significant boost between the 70s and the 80s, when the pioneering investigations by Paczyński (1970) and Schoenberner (1983) first clarified the steps by which the stars, after leaving the asymptotic giant branch (AGB), and consumed almost the entire external envelope, undertake a general contraction, which drives them through the post-AGB, planetary nebulae (PN), and white dwarf evolution. The afore mentioned investigations, of paramount historical importance, were followed by more recent simulations of the AGB-to-PN transition, based on updated physics, proposed by Bloecker (1995) and Miller Bertolami (2016).

The interest towards PNe has raised significantly during the last decade, when it was clarified the notable information that can be drawn from their study, in relation to the previous evolutionary phases, particularly the evolution across the AGB, whose description is made difficult by several uncertainties affecting the knowledge of the underlying physics (Karakas and Lattanzio, 2014). Similarly to the post-AGB counterparts, the PNe are few in number, yet the interpretation of their spectra is free from blending effects caused by molecular lines, thereby facilitating the determination of chemical composition and the derivation of the

most relevant physical parameters of the central star (van Winckel, 2003; Leisy and Dennefeld, 2006).

The traditional modality by which PNe have been used to infer the properties of their progenitors is the comparison of their position on the HR diagram with the evolutionary tracks of model stars of different mass and metallicity. On this regard, Miller Bertolami (2016) presented a database of evolutionary sequences spanning a wide range of core (hence progenitor's) mass and chemical composition, which allows us to infer the physical conditions of the stars upon leaving the AGB and, with some assumptions on the initial-final mass relationship, the progenitor's mass and formation epoch.

A further application of the interpretation of the PNe data, particularly of the surface chemical composition, is the comparison with the final chemical abundances of the AGB computations, which change with the progenitor's mass and metallicity. This is the approach followed by Ventura et al. (2015), Ventura et al. (2016), Ventura et al. (2017), Stanghellini et al. (2022) to characterise samples of PNe in the Magellanic Clouds (MCs) and in the Milky Way, in terms of mass, metallicity and formation epoch of their progenitors.

A further, significant exploration of the opportunities offered by the interpretation of the data of stars evolving through the evolutionary stages following the AGB was based on the analysis of the infrared (IR) excess of the spectra of post-AGB stars. On this regard, Tosi et al. (2022) proposed a novel method, consisting in connecting the IR excess currently observed in the spectra of post-AGB stars with the dust in their surroundings, and to use it to draw information on the dust production which took place in the wind of their progenitors during the final AGB phases, on the time scale of the AGB-to-post-AGB transition, and on the dynamics of the wind leaving the AGB stars, under the push of radiation pressure. This approach, first applied to a sample of post-AGB stars in the LMC, was extended to C-rich and O-rich post-AGB sources in the Galaxy, by Tosi et al. (2023) and Dell'Agli et al. (2023b), respectively.

The final step towards an exhaustive use of PNe as indicators of the previous history of the star was proposed by Dell'Agli et al. (2023a), who showed how also the analysis of the spectra of PNe offers a wide opportunity to derive the physical conditions of the progenitor stars during the final AGB phases, and to shed new light on the dust formation process during the same phases, a key information to assess the role played by AGB stars as dust manufactures in the Universe.

In this contribution we present the recent progresses in the use of the derived properties of PNe as a tool to characterise the progenitors, and discuss how the detailed analysis of their spectra allows to draw information on the variation of the surface chemical composition occurred during the AGB evolution and on the efficiency of the dust formation process during the final AGB phases. The paper is structured as follows: Section 2 gives an overview of the AGB evolution, with the description of the main mechanisms that modify the surface chemical composition and of the process of dust formation in the wind; the potentialities offered by the analysis of the spectral energy distribution of PNe, combined with the results from the modelling of the AGB phase, to reach a global comprehension of the transition from the AGB to the PN phase, are discussed in Section 3. Finally, the conclusions are given in Section 4.

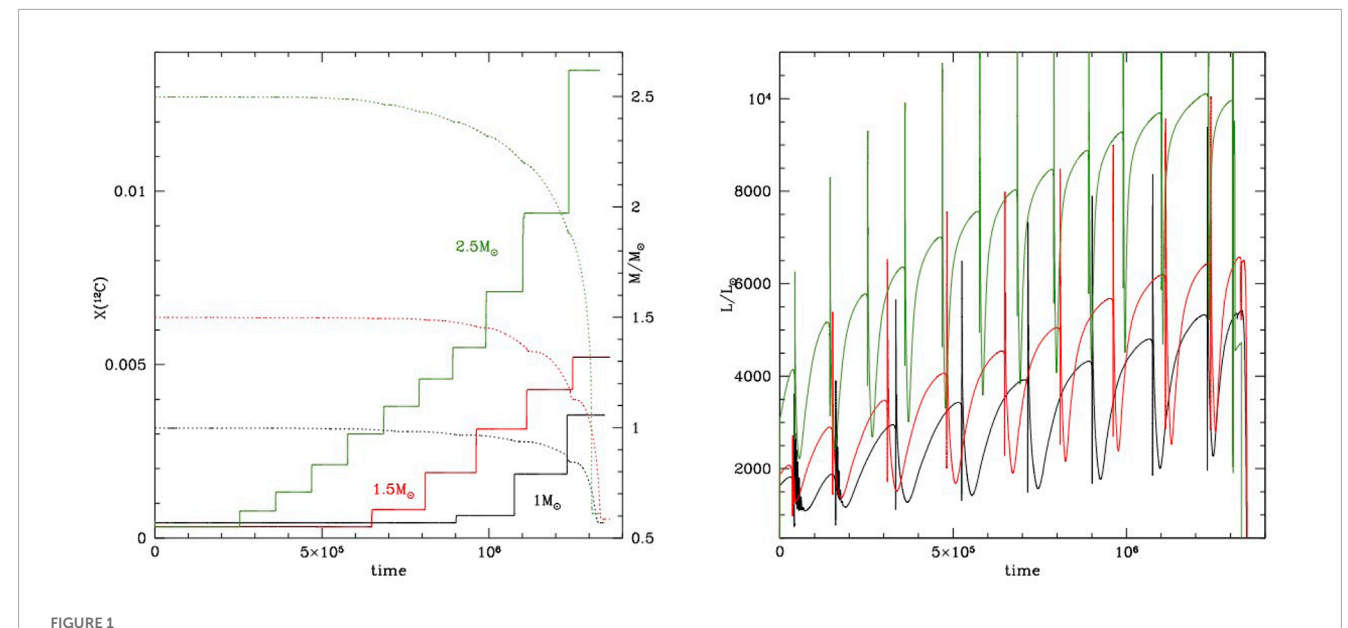
2 The evolution of the stars along the asymptotic giant branch

The interpretation of the observations of PNe and the characterisation of their central star must start from the events that took place during the previous evolutionary phase, the AGB. This is because it is during the AGB phase that the surface chemical composition of the stars is modified, until reaching the distribution of the elements with which they evolve through the PN phase. Also, the dust populating the nebula surrounding the central objects of PNe is an inheritance of the efficient dust formation process taking place in the winds of AGBs. Finally, the luminosity attained during the PN evolution is determined by the rate of growth of the core of the star during the AGB evolution, which, in turn, is related to the rapidity with which the shell CNO burning activity proceeded along the AGB. In this section we describe the most relevant features characterizing the AGB evolution, before entering the discussion on how to interpret the current status of PNe.

The main aspects of the AGB evolution were thoroughly discussed in exhaustive reviews (Iben, 1974; Busso et al., 1999; Herwig, 2005; Karakas and Lattanzio, 2014), which outline that the physical evolution of AGB stars is primarily driven by the core mass, which affects the luminosity (Paczyński, 1970), thus the duration of this evolutionary phase, which span the range extending from a few Myr, for AGB stars descending from solar mass progenitors, to $\sim 10^5$ yr, for $\sim 8\,M_\odot$ stars. The energy output is mainly due to the H-burning nucleosynthesis occurring in a shell above the degenerate core; periodically, helium is ignited in a layer beneath, in conditions of thermal instability (Schwarzschild and Härm, 1965), which is the reason why these episodes are commonly known as thermal pulses (TP). The AGB is halted when the mass of the envelope is reduced to below $\sim 0.01\,M_\odot$, the star contracts, and the post-AGB evolution begins (Miller Bertolami, 2016).

2.1 The evolution of the surface chemistry

The surface chemical composition of AGB stars can be altered by two mechanisms. The first is the third dredge-up (TDU), consisting in the inwards penetration of the base of the convective envelope, which takes place soon after the ignition of the TP (Iben, 1974). During the TDU the surface convection reaches layers of the star previously touched by helium-burning nucleosynthesis, enriched in carbon: repeated TDU events lead to the formation of carbon stars. The other mechanism able to change the chemical composition of the external regions of AGB stars is hot bottom burning (HBB), which consists in the activation of an advanced proton-capture nucleosynthesis at the base of the convective envelope (Boothroyd and Sackmann, 1999; Bloecker and Schoenberner, 1991). The ignition of HBB changes the surface chemistry of the stars according to the equilibria of the proton-capture nucleosynthesis occurring at the bottom of the surface convective zone, in a modality which turns to be extremely sensitive to the metallicity (Z) of the star (Dell'Agli et al., 2018). The activation of HBB requires temperatures at the base of the envelope above 30 MK, which are reached only by stars evolving on core masses above $\sim 0.8 M_{\odot}$, corresponding to $M > 3M_{\odot}$ progenitors (Ventura et al., 2013). On



Time variation of the surface carbon mass fraction (left panel, solid lines, scale on the left), stellar mass (left panel, dotted lines, scale on the right) and luminosity (right panel), of model stars of mass $1M_{\odot}$, $1.5M_{\odot}$, $2.5M_{\odot}$ (black, red and green lines, respectively), from Ventura et al. (2014); the masses of $M \le 2M_{\odot}$ model stars are taken at the start of the core helium burning phase. Times are counted since the start of the thermal pulse phase.

the chemical side, Ventura et al. (2022) identified three main groups of AGB stars, divided according to the modality with which the surface chemical composition changes, which, in turn, reflects the relative efficiency of TDU and HBB: a) low-mass stars; b) carbon stars; c) HBB stars.

Group a) involve stars that begin the core helium burning phase with mass $M < 0.9\,M_\odot$; this threshold mass limit is sensitive to the metallicity, and is lower the lower the Z, with a variation of the order of $0.05\,M_\odot$. The stars belonging to group a) loose the external mantle after experiencing 5-6 TPs. The effects of TDU and HBB are negligible, thus the surface chemistry is altered by the first dredge-up episode only (Charbonnel, 1994), with the consequent increase in the surface N at the expenses of carbon, and the rise in the $^{13}C/^{12}C$ isotopic ratio. These stars are expected to exhibit an oxygen-rich chemistry during the post-AGB and PN phases.

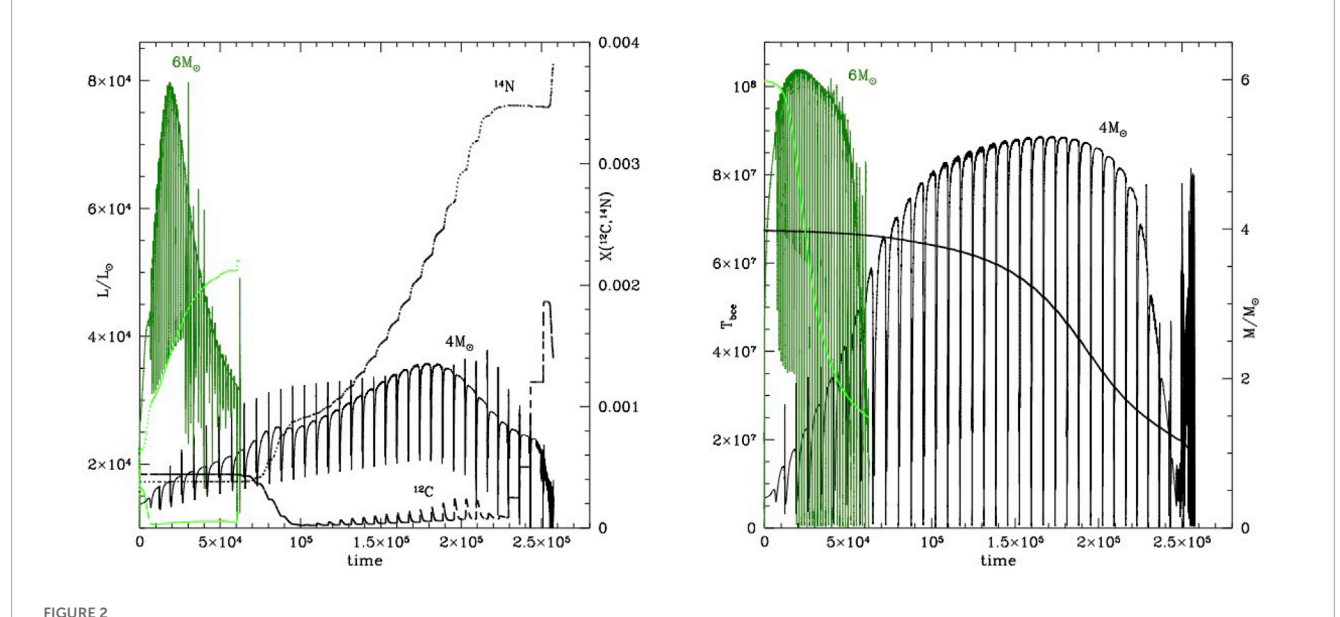
Carbon stars belonging to group b) are the progeny of stars of initial mass in the $1-3\,M_{\odot}$ range, which experience a sufficiently large number of TPs that eventually the surface carbon overcomes oxygen, leading to the C-star stage. A few examples of the evolution of these objects are shown in Figure 1, which refer to model stars of initial mass 1, 1.5, 2.5 M_{\odot} of metallicity $Z = 4 \times 10^{-3}$. The evolutionary sequences reported in the figure, calculated by means of the ATON code for stellar evolution (Mazzitelli, 1979; Ventura et al., 1998), are taken from Ventura et al. (2014). In the left panel of the figure we note the step-like variation of the surface carbon abundance, where each jump reflects the action of a TDU event. The right panel shows the gradual rise in the luminosity, owing the increase in the core mass of the stars, under the action of the H-burning shell; the largest luminosities, of the order of $10^4 L_{\odot}$, are reached during the final AGB phases of the $2.5 M_{\odot}$ model star, as it is the one evolving on the highest core masses.

The formation of carbon stars has a strong effect on the evolution of AGB stars, because it is followed by a significant increase in

the surface molecular opacities (Marigo, 2002), which determines a fast expansion of the external regions (Ventura and Marigo, 2010), with the decrease in the surface gravity, and the enhancement in the rate of mass loss. Therefore, the loss of the external mantle is highly accelerated after the star becomes a carbon star, so the typical situation is that these objects experience an initial AGB phase, during which they evolve as O-rich, followed by a much shorter period, during which they are C-stars. The latter phase is more relevant for the chemical enrichment from these objects, because it is during this phase that most of the envelope loss occurs. This can be seen in the left panel of Figure 1, where it is clear the rapidity with which the mass of the star diminishes after the C-star stage is reached.

The results of Figure 1 show that the final surface carbon abundances, with which these stars evolve into the PN stage, is sensitive to the initial mass of the star, because the higher the mass, the higher the number of TDU events experienced, the larger the accumulation of carbon in the surface regions of the star. In the examples reported in Figure 1 the final mass fraction of ^{12}C are X (^{12}C) = 0.0035, 0.005, 0.0135, for M = 1, 1.5, 2.5 M_{\odot} , respectively.

The stars in group c), descending from M > 3 M_{\odot} progenitors, are characterised by the ignition of HBB. This makes the evolutionary time scales extremely short, because it is accompanied by a significant increase in the luminosity (Bloecker and Schoenberner, 1991), which enhances both the rates with which the core mass grows and the envelope is lost. This is clearly shown in Figure 2, which refers to model stars of initial mass $4M_{\odot}$ and $6M_{\odot}$. We note the tight correlation between the luminosity, L, and the temperature at the bottom of the convective envelope, T_{bce} , and the fast increase in both quantities during the first part of the AGB evolution, until the full ignition of HBB. Both L and T_{bce} decrease during the final part of the AGB lifetime, because HBB is gradually turned off by the loss of the envelope.



Time variation of the luminosity (left panel, solid lines, scale on the left), surface carbon and nitrogen abundances (left panel, scale on the right, dashed and dotted lines, respectively), temperature at the base of the envelope (right panel, scale on the left), stellar mass (right panel, scale on the right) of model stars of initial mass $4M_{\odot}$ (black lines) and $6M_{\odot}$ (green), from Ventura et al. (2014). Times are counted since the start of the thermal pulse phase.

On the chemical side, there is no possibility of reaching the C-star stage in this case, as the intense proton-capture activity at the base of the convective envelope favours the destruction of the surface carbon. Only during the final part of the AGB phase, when HBB is turned-off by the gradual loss of the external mantle, it is possible that a few TDU events might lead to the C/O > 1 condition at the surface of the star, with a carbon excess with respect to oxygen significantly smaller than that reached by the lower mass counterparts belonging to the group b) above.

This is shown in the left panel of Figure 2, where we see the strong depletion of the surface carbon, since the early TPs, and the consequent increase in the nitrogen content of the envelope.

2.2 Dust production

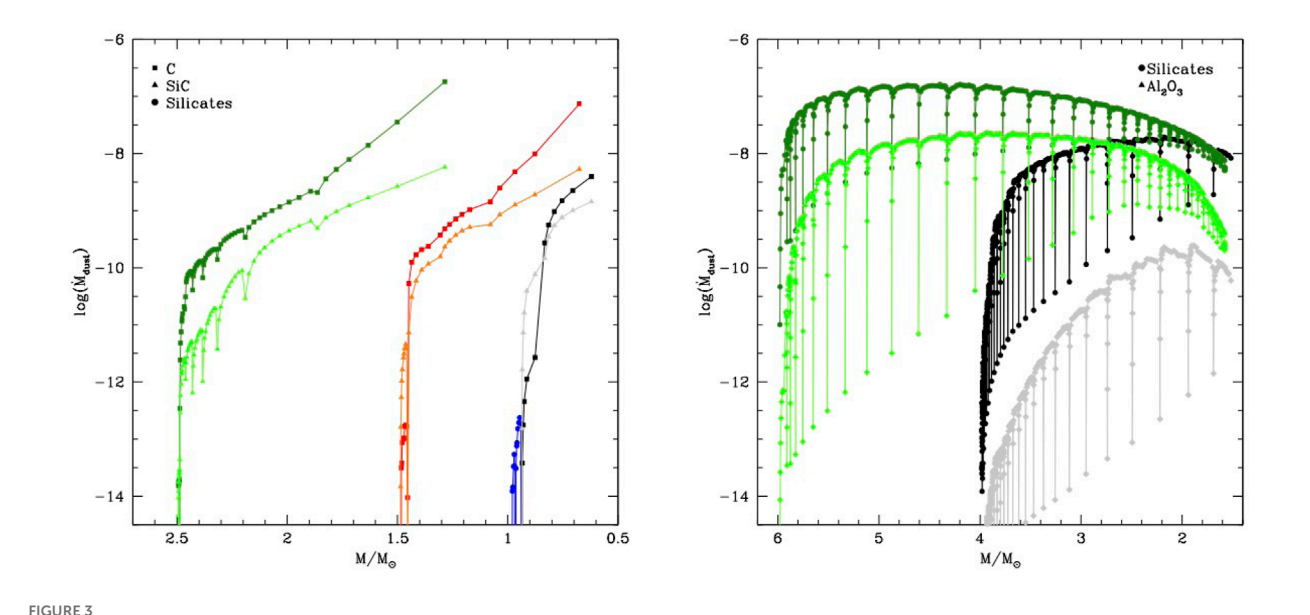
The winds of AGB stars are an environment extremely favourable to the condensation of gaseous molecules into solid particles, owing to the cool temperatures, which inhibit vaporisation, and the large densities (Gail and Sedlmayr, 1985). The Heidelberg team proposed a schematization that can be easily interfaced with results from stellar evolution modelling (Ferrarotti and Gail, 2006) and which was applied by different research groups, to find the dust yields from AGB stars of various mass and metallicity (Ventura et al., 2012; 2014; Nanni et al., 2013; 2014).

The mineralogy of the dust produced during the AGB phase is tightly correlated with the alteration of the surface chemical composition. This is due to the high stability of the CO molecule, which absorbs the least abundant species between carbon and oxygen in its entirety (Ferrarotti and Gail, 2006): in O-rich environments the compounds formed in largest quantities are alumina dust (Al_2O_3) , silicates (olivine - Mg_2SiO_4 , pyroxene - $MgSiO_3$, quartz - SiO_2) and solid iron, whereas in the winds of

carbon stars most of the dust formed is composed by silicon carbide (SiC), solid carbon and solid iron. For each dust species it is defined a key-element, whose abundance drives the rate with which the grains of that specific compound grow and form: this is silicon, for the silicates and SiC, aluminium, for alumina dust, and iron, for solid iron (Ferrarotti and Gail, 2006). In the case of carbon dust the relevant quantity is the carbon excess with respect to oxygen, since the oxygen available absorbs part of the gaseous carbon, in the formation of CO molecules. Independently of the composition of the dust produced, a key ingredient in determining the overall dust production rate (DPR) is the mass loss rate experienced by the star: indeed, for mass conservation reasons, large mass loss rates favour extremely dense winds, thus large numbers of gaseous molecules available to form solid particles.

In relation to the groups a)-c) introduced by Ventura et al. (2022), we find that no carbonaceous species are formed in the wind of the stars in groups a) and c), as they never reach the C-star stage; on the other hand, the AGB evolution of group b) stars is characterised by the initial part, during which alumina dust and silicates are produced, and the second part, when the formation of carbon and SiC dust occurs; solid iron is formed in either cases.

In Figure 3 we show the rates of production of the main dust species, for the stars belonging to the groups b) and c) introduced before. These results were obtained by applying the scheme proposed by Ferrarotti and Gail (2006) to the evolutionary sequences calculated by means of the ATON code, solving the set of equations descrived in Ventura et al. (2012). We do not show any result regarding group a) stars, as little dust is formed in their winds, because the mass loss rates experienced are below or of the order of $10^{-6}\,\dot{M}/\rm yr$, so the winds are not sufficiently dense to allow significant production of dust. The left panel refers to the same model stars shown in Figure 1, whereas on the right we report the 4,6 M_{\odot} model stars discussed in Figure 2. On the abscissa of both panels of Figure 3



The AGB evolution of the dust production rate of carbon dust (squares), SiC (triangles), silicates (circles) and Al_2O_3 (diamonds) of the model stars whose physical and chemical quantities are shown in Figure 1 (left panel) and Figure 2 (right). In the abscissa we report the current mass of the star, decreasing during the AGB lifetime.

we show the (current) mass of the star instead of the time. The reason for this choice is that, particularly for the lowest mass model stars, the C-rich stage is reached only during the very final AGB phases, thus use of time would push this important phase towards the far right side of the figure. Furthermore, use of the current mass facilates the comprehension of the dust yields, which are sensitive not only to the DPR, but also to the mass lost by the star during the evolutionary phases during which dust is produced.

We see in the left panel of Figure 3 that little dust production takes place during the initial part of the AGB evolution of group b) stars, because of the low mass-loss rates, barely reaching $10^{-6} \dot{M}/\text{yr}$. As shown in Figure 3, some production of silicates, with DPR anyway below $10^{-12}\dot{M}/\rm{yr}$, occurs during the O-rich phase of the $1 M_{\odot}$ model star: this is because in this specific case the star evolves as O-rich until the mass of the envelope was reduced to a few tenths of solar masses, so that the low surface gravities favour higher mass loss rates than those experienced during the O-rich phase of its $1.5, 2.5 M_{\odot}$ counterparts. On the contrary, intense production of carbonaceous dust takes place during the C-rich phase of group b) stars, with DPRs as high as $5 \times 10^{-7} \dot{M}/\text{yr}$ during the final AGB phases. The dominant contribution to the overall dust production in group b) stars is provided by solid carbon, with the exception of the evolutionary phases shortly after the stars become C-stars, when the carbon excess to oxygen is smaller than the silicon available. The large rates with which carbon dust is produced during the final part of the AGB evolution of these objects is due to the large quantities of carbon accumulated in the surface regions after the series of TDU events (see left panel of Figure 1), and to the consequent increase in the mass loss rate (Marigo, 2002), which rises the density of the wind. The rate of carbon dust production achieved at the end of the AGB phase increases with the initial mass of the star, because the surface carbon mass fraction also increases with the stellar mass, as shown in the left panel of Figure 1.

Group c) stars never become C-stars, thus the dust formed in their winds is made up of silicates and alumina dust, with traces of solid iron. We see in the right panel of Figure 3 that dust production is particularly strong during the phases of intense HBB, when the luminosities and the mass loss rates reach their maximum values. Silicates are produced at significantly higher rates than alumina dust, despite the latter compound is more stable (Dell'Agli et al., 2014), because of the higher availability of silicon in the surface regions of the star, in comparison to aluminium. The formation of silicates is more efficient in the $6\,M_\odot$ model star than in the $4\,M_\odot$ counterpart, because, as shown in Figure 2, the higher the initial mass of the star, the stronger the HBB conditions reached, the higher the luminosities and the mass loss rates experienced.

We believe important to remark here that the results shown in Figure 3 hold as far as the $Z=4\times10^{-3}$ metallicity is considered. Indeed the intensity of dust production is sensitive to Z, as the latter quantity affects the amount of silicates and alumina dust formed, because the formation of these dust species is determined by the amounts of silicon and aluminium available in the surface regions, which scale linearly with Z. Also the amount of SiC formed is sensitive to the metallicity, since the formation of this compound depends on the silicon surface mass fraction. The only species not deeply affected by the metallicity is carbon dust, because the carbon dredged-up to the surface regions is of primary origin, being sinthesized in the helium burning shell.

2.3 The AGB inheritage

The series of events characterising the AGB lifetime described so far are extremely important to determine the physical and chemical conditions of the stars at the end of the AGB, thus at the beginning of the general contraction process, which will drive them first through

the post-AGB, then the PN stage. Indeed the status of the star when the AGB phase is concluded is the key point to understand the following evolution, considering that the luminosity is substantially unchanged, and the surface chemistry is frozen.

The initial mass of the star, M_{init}, is the key point in establishing the conditions with which the stars undertake the post-AGB path. The luminosities span the $4000-25000\,L_{\odot}$ range: the lower threshold is reached by the lowest masses that reach the AGB phase, i.e., $\sim 0.8 \, M_{\odot}$, whereas the brightest post-AGB stars descend from ~ $8\,M_{\odot}$ progenitors. M_{init} also affects the final surface chemistry, which reflects the combined action of TDU and HBB, whose relative effects change, according to whether the stars belong to the groups a), b) and c), discussed in Ventura et al. (2022). In the case of group a) we expect that the surface nitrogen is increased by a factor from 3 to 5 with respect to the initial abundance, owing to the effects of the first dredge-up, and the surface C is consequently reduced. Some N enhancement is also expected for the stars in group b) that become carbon stars. In this case we also expect significant carbon enhancement, which increases with Minit (see Figure 1). Some oxygen enhancement is also expected, but at a much smaller extent than carbon. The surface chemistry of the stars in group c) is characterized by the carbon and oxygen depletion, and a significant increase in the N content, due to the effects of the proton-capture nucleosynthesis experienced at the base of the convective envelope. Overall, as discussed in Kamath et al. (2023), the carbon content proves the best indicator of the efficiency of the physical processes that modified the chemical composition of the star during the entire AGB lifetime.

Upon leaving the AGB, the stars are surrounded by the dust formed in their wind. M_{init} is once more the key parameter in determining the mineralogy and the amount of dust present in the circumstellar envelopes of the stars, when they start the post-AGB evolution. Low-mass stars that fail to reach the C-star stage (group a) above) and massive AGBs that experience HBB (group c)) are surrounded by silicates and some alumina and iron dust when they depart from the AGB, whereas the stars that become carbon stars will carry on producing carbon dust until the very end of the AGB, with rates sensitive to the initial mass.

3 The connection between PNe and the parent stars

The importance of the study of PNe to probe stellar populations and reconstruct the main properties of the progenitor stars was outlines in several studies presented in the last decades (Stanghellini, 2000; 2006; Buzzoni et al., 2006; Ciardullo, 2006). While most of these studies were based on the interpretation of the position of these objects on the HR diagram and of the derived chemical composition, recent studies have outlined the importance of the dust contained in the PN nebula (Tosi et al., 2024; Ventura et al., 2025). This step is now possible, thanks to the last generation models of the AGB evolution, which also consider the dust formation process, and are able to predict the mineralogy and the rate with which dust is produced during the final AGB phases.

While the main focus here is on the properties of PNe, it is important to mention the new frontier opened in the context of the evolutionary phases following the AGB by the study of Tosi et al. (2022),

who investigated post-AGB sources in the SMC and LMC. The SED of these stars was constructed on the basis of near-IR photometric data taken from the SAGE surveys (Meixner et al., 2006; Gordon et al., 2011), JHK data from the Two Micron All Sky Survey (Skrutskie et al., 2006), and photometry data in the U, V, B and I bands from the Magellanic Clouds Photometric Survey (Zaritsky et al., 2002). The interpretation of these data, based on the comparison with synthetic SED obtained by means of the DUSTY code (Nenkova et al., 1999), showed that the dust properties of post-AGB stars, deduced from the IR excess of their spectral energy distribution (SED), is tightly correlated to the kind of dust now present in the surroundings of the central star. In particular, Tosi et al. (2022) demonstrated the possibility of determining the DPR at the end of the AGB phase and the average velocity with which the gas + dust wind moved away from the surface of the star by the time that star formation stopped, by analyzing the details of the SED. This is of paramount importance in regard of establishing the role that AGB stars play as dust manufactures in the Universe, considering that most of the dust production takes place during the very final AGB phases (see Figure 3), so that the current DPR of galaxies was associated to the very late AGB phases of stars that are about to start the post-AGB evolution (Dell'Agli et al., 2016; 2019). The study by Tosi et al. (2022) was the first exploration in which the knowledge of the main physical and chemical parameters of a post-AGB objects was combined with information regarding the dust composition, to constrain the nature of the progenitor star and to reconstruct the previous history of the star, from the late AGB phases, until the present epoch. The idea proposed by Tosi et al. (2022) for post-AGB stars was extended to investigate the PNe by Dell'Agli et al. (2023a), who stressed the possibility offered by the simultaneous interpretation of photometric and spectroscopic data of sources sharing progenitors of similar mass and chemical composition, to build a bridge connecting the AGB, post-AGB and PN phases, allowing us to reconstruct the series of events occurred since the stars depart from the AGB.

The results from the modelling of the AGB phase and of the dust formation process in the wind, combined with the study by Tosi et al. (2022), give the opportunity of extending the analysis of the observations of PNe beyond the plain characterisation of the individual objects, and to attempt to assemble an overall scenario, connecting the physical and chemical status of the stars before leaving the AGB, with the modality and the intensity of the dust formation process, in relation to the mass, metallicity and formation epoch of the progenitors. These are the ingredients required to describe the dust enrichment from AGB stars in galaxies located at various redshifts, thus formed in different epochs after the Big Bang.

The availability of photometric and spectroscopic data covering a wide spectral interval extending from the UV to the IR proves extremely useful for this kind of analysis, because it makes possible to study the details of the three components of PNe: the central star, the ionized gas, and the dust in the nebula. A first, promising example of this approach was the study by Tosi et al. (2024), who considered a sample of PNe in the LMC, selected on the basis of the availability of the near- and mid-IR spectrum. The detailed analysis of the whole SED leads to the determination of several quantities, such as the parameters of the central star (effective temperature T_{eff} luminosity L), the mass of the gas in the nebula (M_{gas}), the carbon and oxygen abundances, and δ , the dust-to-gas ratio (Tosi et al., 2024).

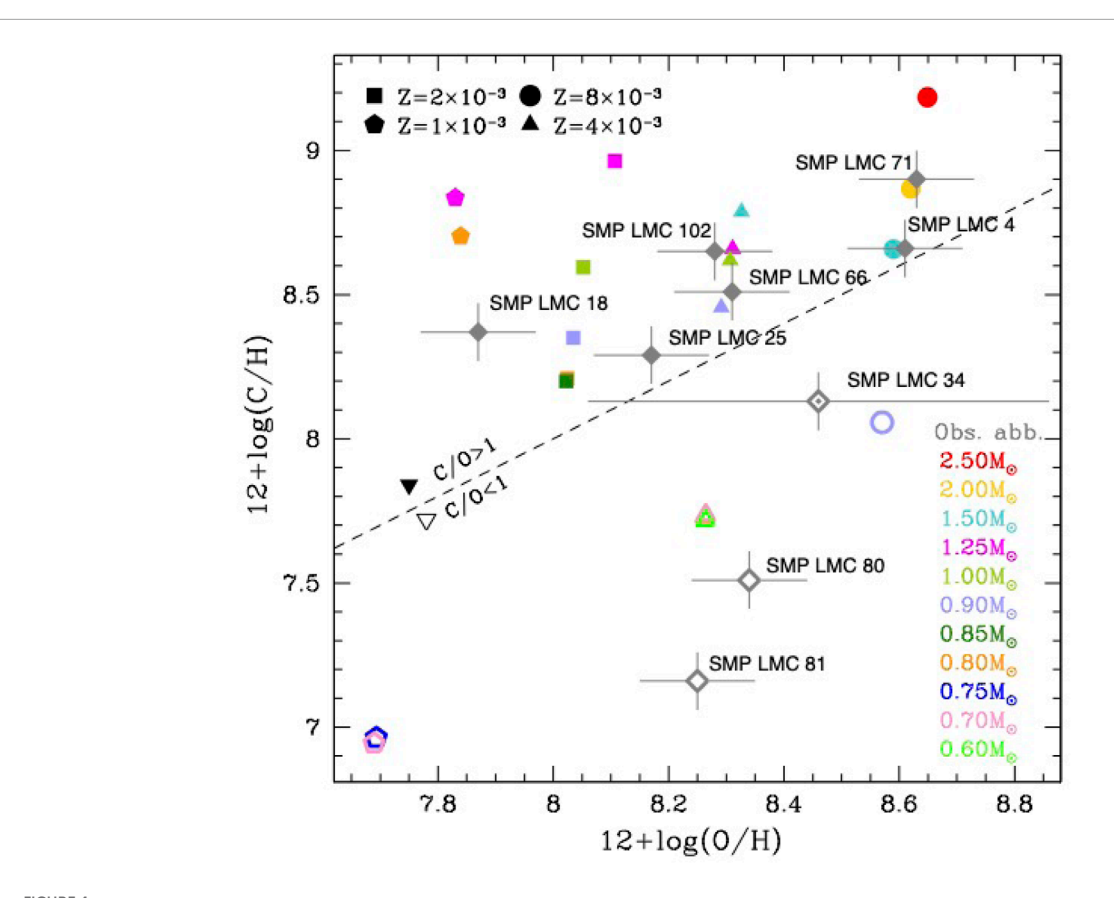
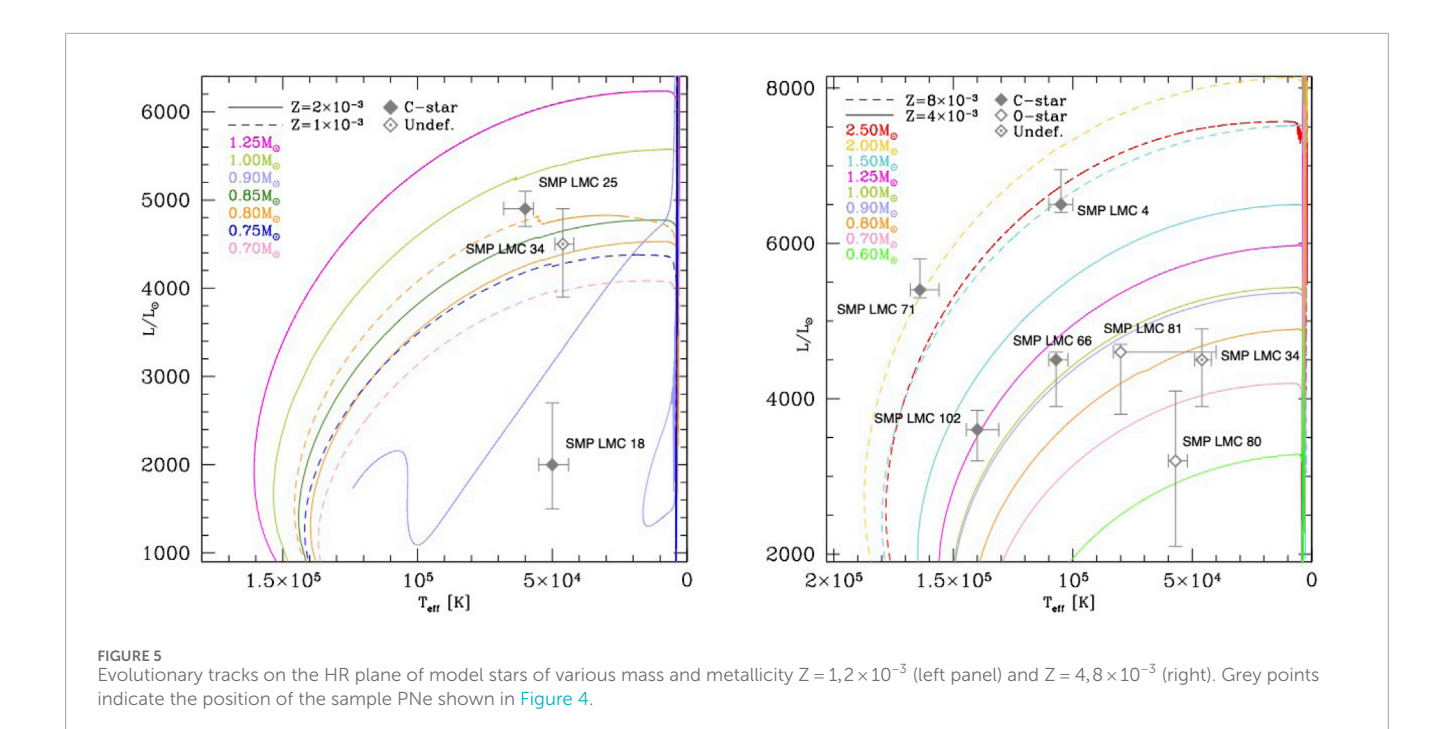


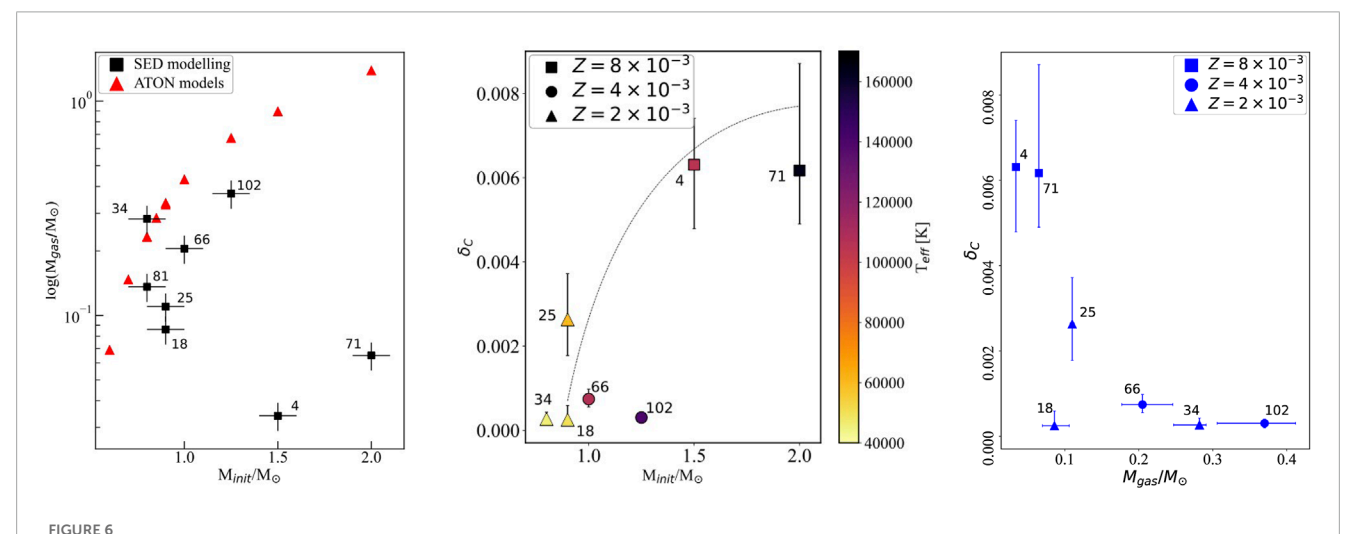
FIGURE 4
Carbon and oxygen abundances (gas phase) of the 9 PNe in the sample considered by Tosi et al. (2024), indicated with grey points, separated in C-rich (full points) and oxygen-rich (open points) sources. No clear chemical tagging was possible for SMP LMC 34, owing to the large uncertainties associated to the oxygen abundance. Coloured points indicate the final abundances of model stars of different mass and chemical composition, calculated by means of the ATON code for stellar evolution, used also for the evolutionary sequences shown in the Figures 1–3.

The first step of this kind of analysis is the search of the progenitor stars of the individual PNe, by comparing the chemical composition of the gas in the nebula, derived from the SED analysis procedure, with the results from AGB evolution modelling, described in Section 2.1. Figure 4 shows the comparison between the final chemical composition of model stars of different mass and metallicity, with the carbon and oxygen abundances derived from the SED analysis procedure. The simultaneous knowledge of the carbon and oxygen content is particularly suitable to this scope, according to the discussion of Section 2.1: the carbon mass fraction is mainly related to the progenitor's mass, while the oxygen content is an indicator of the metallicity (Kamath et al., 2023). The dashed line in the plane separates the O-rich (open points) from the C-rich (full points) chemistries, and allows us to distinguish low-mass stars (SMP LMC 80 and SMP LMC 81 in this example), tentatively associated to the group a) discussed in Section 2, from the higher mass counterparts, which eventually evolve as carbon stars, belonging to the group b) of Section 2. Among others, we note the presence of the source SMP LMC 71, strongly enriched in carbon, identified as the progeny of a $\sim 2 M_{\odot}$ star.

The characterization of the individual stars of the sample is further strenghtened by the comparison between their position on the HR diagram and the evolutionary tracks, calculated for various values of the initial mass and chemical composition. These evolutionary sequences are taken from Ventura et al. (2014) as far as the AGB part is concerned, and were extended to the post-AGB and PNe phases by Marini et al. (2021) and Kamath et al. (2023). This comparison is shown in Figure 5. For clarity sake we separated the tracks of metal poor model stars, reported in the left panel, from those of the sub-solar chemistry counterparts, shown in the right panel. From the combined analysis of the surface chemical composition of the PNe and their position on the HR diagram we conclude that the sample of LMC PNe considered is composed of two metal-poor stars descending from low-mass progenitors (SMP LMC 81 and SMP LMC 81), with an O-rich chemistry, and 7 C-rich objects, of various mass and metallicity, spanning the $0.8 < M_{init} < 2.5\,M_{\odot}$, $10^{-3} < Z < 8 \times 10^{-3}$ ranges.

While the knowledge of the position of the sources on the HR diagram and of their chemical composition leads to the identification of the progenitor stars, interesting information regarding the dust formation process, the survival of the dust formed during the AGB evolution, the dynamics of the gas + dust wind from the end of the AGB until the epoch when the PNe are observed, can be obtained by interpreting the other quantities derived from the SED analysis procedure, related to the gas and dust content of the nebula. We restrict the following discussion to the 7C-rich objects of the PNe sample, given the significant differences in the modality of dust production and in the





The mass of the gas in the nebula and of the dust-to-gas ratio of the C-rich stars in the sample presented in Figure 4 are shown as a function of the derived progenitor's mass in the left and middle panels, respectively. The relationship between the dust-to-gas ratio and the mass of gas is shown in the right panel.

wind dynamics of O-rich and C-rich stars, which complicates any comparative analysis.

The left panel of Figure 6 shows M_{gas} as a function of M_{inii} deduced on the basis of the procedure described above. Black squares indicated the results obtained by means of the SED analysis process, whereas red triangles indicate the mass of the gas released during the last interpulse by model stars of the initial masses reported on the abscissa: the predicted M_{gas} changes from a few tenths of solar masses, for the lowest masses considered here, i.e., $\sim 0.8\,M_{\odot}$, to something around a solar mass for the highest mass $(M\sim 2\,M_{\odot})$ objects. We note substantial agreement between the

values derived from SED analysis and the theoretical expectations for the stars descending from sub-solar mass progenitors, whereas for higher mass stars, such as the sources SMP LMC 4 and SMP LMC 71, the mass of gas currently stored in the nebula is significantly lower than that released during the late interpulse. A possible interpretation of the results shown in the left panel of Figure 6 is that the carbon stars of largest mass, such as the progenitors of SMP LMC 4 and SMP LMC 71, experience a phase of intense dust formation during the final AGB phases (see left panel of Figure 3), which is accompanied by strong radiation pressure, which triggers the dispersion of a significant fraction of the gas released by the star.

This understanding is confirmed by the results shown in the middle and right panels of Figure 6, which show the δ vs. M_{gas} and δ vs. M_{init} relationships. It is clear in the middle panel the anti-correlation pattern between δ and M_{gas} : the sources exhibiting the largest dust-to-gas ratios, of the order of $6-7\times10^{-3}$, are those with the smallest gas mass, below $0.1\,M_{\odot}$. δ is also correlated with the progenitor's mass, as clear in the right panel of Figure 6.

The results reported in Figure 6 are consistent with our understanding of the dust formation process during the AGB evolution and the events occurring since the start of the post-AGB phase. The sources exhibiting the largest amount of carbon dust in relation to the gas content of the nebula are those descending from the progenitors of highest mass, consistently with the results discussed in Section 2.2. In these stars we expect an enhanced effect of the radiation pressure, which is the motivation for the derived small gas contents. The large δ 's are due to the large DPR's experienced during the final AGB phases, and to the dispersion of large fractions of gas, which contributes to rise the dust-to-gas ratio.

In the right panel of Figure 6 we report with a cyan line a rough pattern relating the progenitor's mass of the PNe in the sample and the dust-to-gas ratio: this trend extends from almost null values of δ , for M ~ 0.8 M_{\odot} , to δ ~ 0.008, for M ~ 2 M_{\odot} . The sources SMP LMC 102 and SMP LMC 71 are located below the average trend, which indicates a content of dust currently located in the nebula below the expectations. A possible explanation for these deviations is that these two sources are the hottest in the sample (see the temperature scale on the right hand side of the panel), which might have favoured the vaporisation of part of the dust in the nebula.

4 Conclusion

We discuss how results from AGB evolution and dust formation modelling can be used to interpret multi-band observations of PNe, which allow inspection of the different components, from the central star, to the nebula. We show the potentialities of adopting a two-steps procedure, where the traditional method to study the PNe, based on the knowledge of the parameters of the central object and of the chemical composition of the gas, is completed with the interpretation of the other quantities derived from SED analysis, related to the gas and dust content of the nebula.

The position of the stars on the HR diagram and the carbon and oxygen abundances of the gas in the nebula allow the identification of the progenitor star, by comparing these data with the evolutionary tracks of stars and with the results from AGB modelling of stars of various mass and chemical composition, particularly of the luminosity and the chemical composition upon leaving the AGB. The detailed analysis of the SED leads to the determination of further quantities, primarily the mass of the gas stored in the nebula and the dust-to-gas ratio, which can be correlated to the dust formation that took place during the final AGB phases, thus compared with the results from the description of dust formation in the wind of AGB stars.

We discuss the results obtained for a sample of PNe in the LMC, which seem to confirm the scenario set up in the last years in regard of dust formation by AGB stars. The gas-to-dust ratio is found to be higher, slightly below 1%, in the PNe descending from $\sim 2\,M_{\odot}$ progenitors, which are believed to be among the most efficient carbon dust manufactures. We find an interesting anticorrelation

pattern connecting this dust-to-gas ratio with the mass currently stored in the nebula, which might suggest an easier dispersion of gas from the stars producing large quantities of dust, a possible signature of enhanced radiation pressure effects.

A promising outcome of these studies is the definition of patterns connecting the dust and gas properties of the PNe with the parten stars, which will open the way to a more ribust identification of the progenitor stars with respect to the status of the art, and to shed new light on the efficiency of dust formation characterizing the late AGB phases, those most important to assess the role of these low and intermediate mass stars as dust manufacturers.

Author contributions

PV: Writing – review and editing. ST: Formal Analysis, Writing – review and editing, Methodology. FD: Conceptualization, Writing – original draft. SB: Writing – review and editing.

Funding

The author(s) declare that no financial support was received for the research and/or publication of this article.

Acknowledgements

PV acknowledges support by the INAF-Theory-GRANT 2022 "Understanding mass loss and dust production from evolved stars". ST acknowledges support from the INAF research project LBT-Supporto Arizona Italia.

Conflict of interest

The authors declare that the research was conducted in the absence of any commercial or financial relationships that could be construed as a potential conflict of interest.

Generative AI statement

The author(s) declare that no Generative AI was used in the creation of this manuscript.

Any alternative text (alt text) provided alongside figures in this article has been generated by Frontiers with the support of artificial intelligence and reasonable efforts have been made to ensure accuracy, including review by the authors wherever possible. If you identify any issues, please contact us.

Publisher's note

All claims expressed in this article are solely those of the authors and do not necessarily represent those of their affiliated

organizations, or those of the publisher, the editors and the reviewers. Any product that may be evaluated in this article, or claim that may be made by its manufacturer, is not guaranteed or endorsed by the publisher.

References

Bloecker, T. (1995). Stellar evolution of low- and intermediate-mass stars. II. Post-AGB evolution. *Astronomy and Astrophysics* 299, 755.

Bloecker, T., and Schoenberner, D. (1991). A 7M AGB model sequence not complying with the core mass-luminosity relation. Astronomy and Astrophysics 244, L43–L46.

Boothroyd, A. I., and Sackmann, I. J. (1999). The CNO isotopes: deep circulation in red giants and first and second Dredge-up. *Astrophysical J.* 510, 232–250. doi:10.1086/306546

Busso, M., Gallino, R., and Wasserburg, G. J. (1999). Nucleosynthesis in asymptotic giant branch stars: relevance for galactic enrichment and solar system formation. Annu. Rev. Astronomy and Astrophysics 37, 239–309. doi:10.1146/annurev.astro. 37.1.239

Buzzoni, A., Arnaboldi, M., and Corradi, R. L. M. (2006). Planetary nebulae as tracers of galaxy stellar populations. *Mon. Notices R. Astronomical Soc.* 368, 877–894. doi:10.1111/j.1365-2966.2006.10163.x

Charbonnel, C. (1994). Clues for non-standard mixing on the red giant branch from 12C/13C and 12C/14N ratios in evolved stars. *Astronomy and Astrophysics* 282, 811–820

Ciardullo, R. (2006). Planetary nebulae as probes of stellar populations. In *Planetary Nebulae in our Galaxy and Beyond*, eds. M. J. Barlow, and R. H. Méndez 234 (Cambridge: Cambridge University Press) IAU Symposium, Waikaloa, Hawaii, 325–332. doi:10.1017/S1743921306003164

Dell'Agli, F., García-Hernández, D. A., Rossi, C., Ventura, P., Di Criscienzo, M., and Schneider, R. (2014). On the alumina dust production in the winds of O-rich asymptotic giant branch stars. *Mon. Notices R. Astronomical Soc.* 441, 1115–1125. doi:10.1093/mnras/stu647

Dell'Agli, F., Di Criscienzo, M., Boyer, M. L., and García-Hernández, D. A. (2016). Evolved stars in the local group galaxies - I. AGB evolution and dust production in IC 1613. *Mon. Notices R. Astronomical Soc.* 460, 4230–4241. doi:10.1093/mnras/stw1276

Dell'Agli, F., García-Hernández, D. A., Ventura, P., Mészáros, S., Masseron, T., Fernández-Trincado, J. G., et al. (2018). A view of the H-band light-element chemical patterns in globular clusters under the AGB self-enrichment scenario. *Mon. Notices R. Astronomical Soc.* 475, 3098–3116. doi:10.1093/mnras/stx3249

Dell'Agli, F., Di Criscienzo, M., García-Hernández, D. A., Ventura, P., Limongi, M., Marini, E., et al. (2019). Evolved stars in the local group galaxies - III. AGB and RSG stars in sextans A. *Mon. Notices R. Astronomical Soc.* 482, 4733–4743. doi:10.1093/mnras/sty2727

Dell'Agli, F., Tosi, S., Kamath, D., Stanghellini, L., Bianchi, S., Ventura, P., et al. (2023a). Dust from evolved stars: a pilot analysis of the AGB to PN transition. *Mon. Notices R. Astronomical Soc.* 526, 5386–5392. doi:10.1093/mnras/stad3080

Dell'Agli, F., Tosi, S., Kamath, D., Ventura, P., Van Winckel, H., Marini, E., et al. (2023b). Study of oxygen-rich post-AGB stars in the Milky Way as a means to explain the production of silicates among evolved stars. *Astronomy and Astrophysics* 671, A86. doi:10.1051/0004-6361/202245250

Ferrarotti, A. S., and Gail, H. P. (2006). Composition and quantities of dust produced by AGB-stars and returned to the interstellar medium. *Astronomy and Astrophysics* 447, 553–576. doi:10.1051/0004-6361:20041198

Gail, H. P., and Sedlmayr, E. (1985). Dust formation in stellar winds. II - carbon condensation in stationary, spherically expanding winds. *Astronomy and Astrophysics* 148, 183–190.

Gordon, K. D., Meixner, M., Meade, M. R., Whitney, B., Engelbracht, C., Bot, C., et al. (2011). Surveying the agents of galaxy evolution in the tidally stripped, low metallicity Small Magellanic Cloud (SAGE-SMC). I. Overview. *Astronomical J.* 142, 102. doi:10.1088/0004-6256/142/4/102

Herwig, F. (2005). Evolution of asymptotic giant branch stars. Annu. Rev. Astronomy and Astrophysics 43, 435–479. doi:10.1146/annurev.astro.43.072103.150600

Iben, I., Jr. (1974). Post main sequence evolution of single stars. *Annu. Rev. Astronomy and Astrophysics* 12, 215–256. doi:10.1146/annurev.aa.12.090174.001243

Kamath, D., Dell'Agli, F., Ventura, P., Van Winckel, H., Tosi, S., and Karakas, A. I. (2023). Modelling of the post-asymptotic giant branch phase as a tool to understand asymptotic giant branch evolution and nucleosynthesis. *Mon. Notices R. Astronomical Soc.* 519, 2169–2185. doi:10.1093/mnras/stac3366

Karakas, A. I., and Lattanzio, J. C. (2014). The dawes review 2: nucleosynthesis and stellar yields of low- and intermediate-mass single stars. *Publ. Astronomical Soc. Aust.* 31, e030. doi:10.1017/pasa.2014.21

Leisy, P., and Dennefeld, M. (2006). Planetary nebulae in the magellanic clouds. II. Abundances and element production. *Astronomy and Astrophysics* 456, 451–466. doi:10.1051/0004-6361:20053063

Marigo, P. (2002). Asymptotic giant branch evolution at varying surface C/O ratio: effects of changes in molecular opacities. *Astronomy and Astrophysics* 387, 507–519. doi:10.1051/0004-6361:20020304

Marini, E., Dell'Agli, F., Groenewegen, M. A. T., García-Hernández, D. A., Mattsson, L., Kamath, D., et al. (2021). Understanding the evolution and dust formation of carbon stars in the Large Magellanic Cloud via the JWST. Astronomy and Astrophysics 647, A69. doi:10.1051/0004-6361/202039613

Mazzitelli, I. (1979). Solar models, helium content and mixing length. Astronomy and Astrophysics 79, 251–253.

Meixner, M., Gordon, K. D., Indebetouw, R., Hora, J. L., Whitney, B., Blum, R., et al. (2006). Spitzer survey of the Large Magellanic Cloud: surveying the agents of a galaxy's evolution (SAGE). I. Overview and initial results. *Astronomical J.* 132, 2268–2288. doi:10.1086/508185

Miller Bertolami, M. M. (2016). New models for the evolution of post-asymptotic giant branch stars and central stars of planetary nebulae. *Astronomy and Astrophysics* 588, A25. doi:10.1051/0004-6361/201526577

Nanni, A., Bressan, A., Marigo, P., and Girardi, L. (2013). Evolution of thermally pulsing asymptotic giant branch stars - II. Dust production at varying metallicity. *Mon. Notices R. Astronomical Soc.* 434, 2390–2417. doi:10.1093/mnras/stt1175

Nanni, A., Bressan, A., Marigo, P., and Girardi, L. (2014). Evolution of thermally pulsing asymptotic giant branch stars - III. Dust production at supersolar metallicities. *Mon. Notices R. Astronomical Soc.* 438, 2328–2340. doi:10.1093/mnras/stt2348

Nenkova, M., Ivezic, Z., and Elitzur, M. (1999). "DUSTY: a publicly available code for continuum radiative transfer in astrophysical environments," in *Thermal emission spectroscopy and analysis of dust, disks, and regoliths*. Editors A. Sprague, D. K. Lynch, and M. Sitko (Houston: LPI Contributions), 969.

Paczyński, B. (1970). Evolution of single stars. I. Stellar evolution from main sequence to white dwarf or carbon ignition. *Acta Astron.* 20, 47.

Schoenberner, D. (1983). Late stages of stellar evolution. II. Mass loss and the transition of asymptotic giant branch stars into hot remnants. *Astrophysical J.* 272, 708–714. doi:10.1086/161333

Schwarzschild, M., and Härm, R. (1965). Thermal instability in non-degenerate stars. $A strophysical\ J.\ 142,855.\ doi:10.1086/148358$

Skrutskie, M. F., Cutri, R. M., Stiening, R., Weinberg, M. D., Schneider, S., Carpenter, J. M., et al. (2006). The two micron all sky survey (2MASS). *Astronomical J.* 131, 1163–1183. doi:10.1086/498708

Stanghellini, L. (2000). "Planetary nebulae as probes of stellar evolution and populations," in *Astrophysics and space science library*. Editors F. Matteucci, and F. Giovannelli (Dordrecht: Kluwer Academic Publisher), 255, 93–100. doi:10.1007/978-94-010-0938-6 9

Stanghellini, L. (2006). "Magellanic cloud planetary nebulae as probes of stellar evolution and populations," in *The local group as an astrophysical laboratory*. Editors M. Livio, and T. M. Brown, 17, 196–207. doi:10.1017/cbo9780511734908.014

Stanghellini, L., Bushra, R., Shaw, R. A., Dell'Agli, F., García-Hernández, D. A., and Ventura, P. (2022). Carbon abundances in compact galactic planetary nebulae: an ultraviolet spectroscopic study with the space telescope imaging spectrograph (STIS). Astrophysical J. 929, 148. doi:10.3847/1538-4357/ac5d50

Tosi, S., Dell'Agli, F., Kamath, D., Ventura, P., Van Winckel, H., and Marini, E. (2022). Understanding dust production and mass loss in the AGB phase using post-AGB stars in the magellanic clouds. *Astronomy and Astrophysics* 668, A22. doi:10.1051/0004-6361/202244222

Tosi, S., Kamath, D., Dell'Agli, F., Van Winckel, H., Ventura, P., Marchetti, T., et al. (2023). A study of carbon-rich post-AGB stars in the Milky Way to understand the production of carbonaceous dust from evolved stars. *Astronomy and Astrophysics* 673, A41. doi:10.1051/0004-6361/202245563

Tosi, S., Dell'Agli, F., Kamath, D., Stanghellini, L., Ventura, P., Bianchi, S., et al. (2024). Planetary nebulae of the Large Magellanic Cloud. I. A multiwavelength analysis. *Astronomy and Astrophysics* 688, A36. doi:10.1051/0004-6361/202449588

van Winckel, H. (2003). Post-AGB stars. Annu. Rev. Astronomy and Astrophysics 41, 391–427. doi:10.1146/annurev.astro.41.071601.170018

Ventura, P., and Marigo, P. (2010). Asymptotic giant branch stars at low metallicity: the challenging interplay between the mass-loss and molecular opacities. *Mon. Notices R. Astronomical Soc.* 408, 2476–2486. doi:10.1111/j.1365-2966.2010. 17304.x

Ventura, P., Zeppieri, A., Mazzitelli, I., and D'Antona, F. (1998). Full spectrum of turbulence convective mixing: I. Theoretical main sequences and turn-off for 0.6 - 15 Msun. *Astronomy and Astrophysics* 334, 953–968.

Ventura, P., di Criscienzo, M., Schneider, R., Carini, R., Valiante, R., D'Antona, F., et al. (2012). The transition from carbon dust to silicate production in low-metallicity asymptotic giant branch and super-asymptotic giant branch stars. *Mon. Notices R. Astronomica Soc.* 420, 1442–1456. doi:10.1111/j.1365-2966.2011. 20129.x

Ventura, P., Di Criscienzo, M., Carini, R., and D'Antona, F. (2013). Yields of AGB and SAGB models with chemistry of low- and high-metallicity globular clusters. *Mon. Notices R. Astronomica Soc.* 431, 3642–3653. doi:10.1093/mnras/stt444

Ventura, P., Dell'Agli, F., Schneider, R., Di Criscienzo, M., Rossi, C., La Franca, F., et al. (2014). Dust from asymptotic giant branch stars: relevant factors and modelling uncertainties. *Mon. Notices R. Astronomica Soc.* 439, 977–989. doi:10.1093/mnras/stu028

Ventura, P., Stanghellini, L., Dell'Agli, F., García-Hernández, D. A., and Di Criscienzo, M. (2015). A test for asymptotic giant branch evolution theories: planetary nebulae in the Large Magellanic Cloud. *Montlhy Notices R. Astronomical Soc.* 452, 3679–3688. doi:10.1093/mnras/stv1590

Ventura, P., Stanghellini, L., Di Criscienzo, M., García-Hernández, D. A., and Dell'Agli, F. (2016). Planetary nebulae in the Small Magellanic Cloud. *Montlhy Notices R. Astronomical Soc.* 460, 3940–3949. doi:10.1093/mnras/stw1254

Ventura, P., Stanghellini, L., Dell'Agli, F., and García-Hernández, D. A. (2017). The evolution of galactic planetary nebula progenitors through the comparison of their nebular abundances with AGB yields. *Montlhy Notices R. Astronomical Soc.* 471, 4648–4661. doi:10.1093/mnras/stx1907

Ventura, P., Dell'Agli, F., Tailo, M., Castellani, M., Marini, E., Tosi, S., et al. (2022). Nucleosynthesis, mixing processes, and gas pollution from AGB stars. *Universe* 8, 45. doi:10.3390/universe8010045

Ventura, P., Tosi, S., García-Hernández, D. A., Dell'Agli, F., Kamath, D., Stanghellini, L., et al. (2025). Planetary nebulae of the Large Magellanic Cloud: II. The connection with the progenitors' properties. *Astronomy and Astrophysics* 694, A177. doi:10.1051/0004-6361/202452188

Zaritsky, D., Harris, J., Thompson, I. B., Grebel, E. K., and Massey, P. (2002). The magellanic clouds photomtric survey: the Small Magellanic Cloud stellar catalog and extinction map. *Astronomical J.* 123, 855–872. doi:10.1086/338437